

# Folding of Alzheimer's core PHF subunit revealed by monoclonal antibody 423

Rostislav Skrabana<sup>a</sup>, Peter Kontsek<sup>a</sup>, Anna Mederlyova<sup>b</sup>, Khalid Iqbal<sup>c,\*</sup>, Michal Novak<sup>b,\*</sup>

<sup>a</sup>Axon Neuroscience, Rennweg 95b, 1030 Vienna, Austria

<sup>b</sup>Institute of Neuroimmunology, Slovak Academy of Sciences, Dubravská cesta 9, 845 10 Bratislava, Slovakia

<sup>c</sup>New York State Institute for Basic Research in Developmental Disabilities, Staten Island, NY 10314, USA

Received 10 March 2004; revised 28 April 2004; accepted 29 April 2004

Available online 31 May 2004

Edited by Thomas L. James

Dedicated to the late Caesar Milstein, who was instrumental for this study

**Abstract** At present, the conformation-dependent monoclonal antibodies (mAb) provide the only information on folding of tau in the core PHF. Monoclonal antibody MN423 recognizes all and only those Alzheimer's disease (AD) core paired helical filaments (PHFs) subunits, which terminate at Glu391. Using recombinant analogs of the core PHF subunit corresponding to tau residues  $\tau$ 297–391, we found that the C-terminal pentapeptide <sup>387</sup>DHGAE<sup>391</sup> represented only one component of the structure recognized by mAb 423. Therefore, deletion mutants of the core subunit were generated to identify assembled parts of this conformational structure. We localized two spatially close components in the region 306–325 (<sup>306</sup>VQIVYK<sup>311</sup> and <sup>321</sup>KCGSL<sup>325</sup>) contributing to formation of the structure identified by mAb 423. Thus, the spatial proximity of three subunit segments <sup>306</sup>VQIVYK<sup>311</sup>, <sup>321</sup>KCGSL<sup>325</sup> and <sup>387</sup>DHGAE<sup>391</sup> represents constraints for intramolecular folding of the core PHF subunit. Since PHF represents a compelling drug target in AD, structural knowledge presented could contribute to structure-based drug design.

© 2004 Published by Elsevier B.V. on behalf of the Federation of European Biochemical Societies.

**Keywords:** Alzheimer's disease; Tau protein; Truncation; Paired helical filament

## 1. Introduction

The abnormal hyperphosphorylation and polymerization of the tau protein into paired helical filaments (PHFs) is a seminal event in the pathogenesis of Alzheimer's disease (AD). It is broadly accepted that tau dysfunction causes neurodegeneration, with the formation of tau filaments in AD [1–4]. While all the available data suggest that normal tau has no discrete structure, the presence of highly ordered tau as-

semblies (e.g., PHF) in AD indicates that, in the disease state, tau can and does adopt a different conformation. Proteolytic cleavage dissected Alzheimer's PHF into two structurally distinct parts: protease-sensitive fuzzy coat and a protease-resistant PHF (termed core PHF), which retained its characteristic morphological features [5]. This implicated that the structure of core PHF should be of fundamental importance in the process of tau polymerization. Considerable effort has been aimed at understanding the structure of the pathological tau in PHF [6]. Inherent physicochemical properties of tau preclude conformational analysis of PHF by X-ray crystallography or NMR spectroscopy. In such situation, well-characterized antibodies provide invaluable tool to assess the protein folding if they recognize conformational epitope. The generation of conformation-dependent antibodies provides evidence that tau, a natively unfolded protein [7], is capable of undergoing conformational changes upon polymerization into highly ordered filaments during the course of AD [8–12].

Monoclonal antibody 423 recognizes a three dimensional structure which is specific for tau assembled into PHF in brains of patients with AD but is not present in normal brains [13]. Since previous studies demonstrated that the epitope of 423 is conformational [8,11], phosphorylation independent [8,13] and core PHF specific [8,14–16], its full molecular mapping could significantly contribute to unraveling the molecular basis of PHF formation in AD. Doing this, present work represents first structural insight into folding of core PHF subunit.

## 2. Materials and methods

### 2.1. Preparation, expression and purification of core PHF subunit dGAE and its deletion mutants

The preparation of cDNA coding for core PHF subunit dGAE (residues  $\tau$ 297–391) was described elsewhere [16]. The numbering of amino acids is that of the isoform human  $\tau$ 40 containing 441 residues [17]. For primary structure of dGAE subunit, see Fig. 1. dGAE mutants with amino-terminal deletions ( $\tau$ 306–391,  $\tau$ 316–391,  $\tau$ 321–391 and  $\tau$ 326–391) (see Fig. 3A) were derived from cDNA dGAE by PCR using specific primers. dGAE-mutants with internal deletions [(dGAE $\Delta$ I, dGAE $\Delta$ II, dGAE $\Delta$ III, dGAE $\Delta$ (I+II), and dGAE $\Delta$ (I+III)] (see Fig. 4A) were derived from cDNA dGAE by inverse PCR with inverted primers flanking the deleting sequence. All DNA constructs were cloned in *pET17b* vector (Novagen) through *NdeI*–*EcoRI* restriction sites. Integrity of each construct was verified by DNA sequence analysis (ABI Prism 377 DNA Sequencer, Perkin–Elmer).

\*Corresponding authors. Fax: +1-718-494-1080 (K. Iqbal), +421-2-54774276 (M. Novak).

E-mail addresses: iqbal@worldnet.att.net (K. Iqbal), Michal.Novak@savba.sk (M. Novak).

**Abbreviations:** AD, Alzheimer's disease; ECL, enhanced chemiluminescence; ELISA, enzyme linked immunosorbent assay; mAb, monoclonal antibody; NMR, nuclear magnetic resonance; PBS, phosphate buffered saline; PHF, paired helical filaments; SDS–PAGE, sodium dodecyl sulfate–polyacrylamide gel electrophoresis

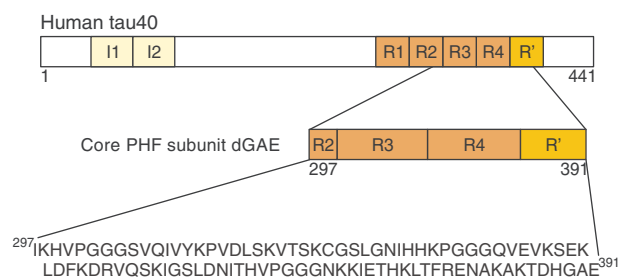


Fig. 1. Structure diagram of core PHF subunit dGAE and its amino acid sequence. Numbering follows that of the human tau40 [17]. I1, I2 – aminoterminal inserts, R1–4, R' – repeat regions.

DNA constructs were expressed in *Escherichia coli* and purified from bacterial lysates (without acid and boiling pretreatment) by one step cation exchange chromatography [18]. The purity of proteins analyzed by SDS–PAGE was more than 90% (data not shown). The protein concentration was determined by scanning densitometry of Coomassie Brilliant Blue stained polyacrylamide gels (data not shown) using program UnScanItGel (SilkScientific Corp., USA).

Synthetic oligopeptides corresponding to the sequences of tau <sup>387</sup>DHGAE<sup>391</sup> and <sup>382</sup>AKAKTDHGAE<sup>391</sup> (purity >95%) were purchased from Interactiva, Germany.

## 2.2. MAb and competitive immunoassay

Monoclonal antibodies (mAb) 423 was raised against an enriched preparation of PHFs [14]. Antibody was purified from ascitic fluid and conjugated with horseradish peroxidase (KemEnTec, Denmark).

The competitive ELISA against solid phase was performed in flexible microtitration plates (Becton Dickinson, Cat. No. 3912, USA) as follows: The competition plate was coated with 50 µl/well of dGAE (18.8 nM) in phosphate buffered saline (PBS), pH 7.2, and then incubated overnight at 4 °C. On the separate plate, serially diluted competitors in PBS were mixed with peroxidase-labeled mAb 423 (0.4 mg/ml). 50 µl per well of the competitor-antibody mixtures was transferred in triplicate to the blocked and washed competition plate and incubated at 37 °C for 35 min. Bound labeled mAb 423 was detected with orthophenylenediamine (Sigma) and plates were read at 492 nm in an iEMS Reader (Labsystems, Finland).

Competition curves for each peptide were fitted using four parameter logistic algorithm and computed and plotted using GraphPad Prism version 3.02 for Windows (GraphPad Software, USA). The values of EC<sub>50</sub> (the effective concentration of half-maximal competition) were calculated, which reflect the antibody affinity [19]. Ratio between EC<sub>50</sub> of respective peptide and EC<sub>50</sub> of dGAE was designated as *r*. It indicates relative decrease (*r*-fold) in affinity of peptide in relation to full affinity of dGAE. All quantitative experimental results shown are from measurement done in triplicate. Error bars in figures represent standard error of the mean.

## 2.3. Immunoelectron microscopy

Immunoelectron microscopy of pronase-treated PHFs with mAb 423 was carried out as described [5,6]. Human AD brain tissue was obtained from Slovak Brain Bank (Bratislava).

## 2.4. SDS–PAGE and western blotting

The core PHF subunit (dGAE) and its deletion mutants were analyzed on SDS–PAGE and Western blot as described previously [18]. ECL developed Western blot was digitalized with LAS3000 CCD imaging system (Fujifilm, Japan). Densitometric data analysis and relative quantification of Western blot record were performed by AIDA Biopackage (Raytest, Germany) as described [18].

## 3. Results and discussion

While the exact molecular structure of both the normal and AD pathological conformation of tau remains to be elucidated, it has been shown that both conformations do exist as discrete molecular entities [8]. Intramolecular interactions in

the core PHF subunits are largely unknown. Therefore, we exploited conformation-dependent mAb 423 as an effective tool for the identification of spatially proximal segments in core PHF subunits which define constraints for folding into mAb 423-specific antigenic structure. Analogical strategy for determination of tau folding during early PHF formation was recently employed in studies with conformational-dependent mAbs Alz-50, MC-1, TG-3 and Tau-66 [9,10,12]. These authors, however, used only qualitative immunochemical methods (Western blot, ELISA) for folding analysis. In contrast, we employed sensitive quantitative competitive ELISA, which allows precise determination of the contribution of individual polypeptide segments to the folding of the core PHF tau. For this study, recombinant core PHF subunit analog termed dGAE corresponding to tau residues τ297–391 (Fig. 1) was used as a representative core subunit.

### 3.1. Affinity of the mAb 423 to the C-terminal regions of core PHF subunit

Previous study of the core PHF subunits identified the C-terminal glutamic acid at position 391 as crucial for adopting the local specific conformation recognized by mAb 423 [16]. The removal or addition of a single amino acid to the C-terminus (Glu391) abolishes the reactivity with mAb 423, suggesting that it has an absolute requirement for a free carboxy terminus. However, this result did not provide an answer to the question whether this C-terminal residue has only structural role or it is also involved in direct interaction with the antibody. To outline this, synthetic peptides were derived from C-terminal region of dGAE and then were assessed for binding with mAb 423 in competitive ELISA using dGAE subunit as a competitor (Fig. 2). Affinity comparisons showed that C-terminal pentapeptide <sup>387</sup>DHGAE<sup>391</sup> of the core subunit exhibited

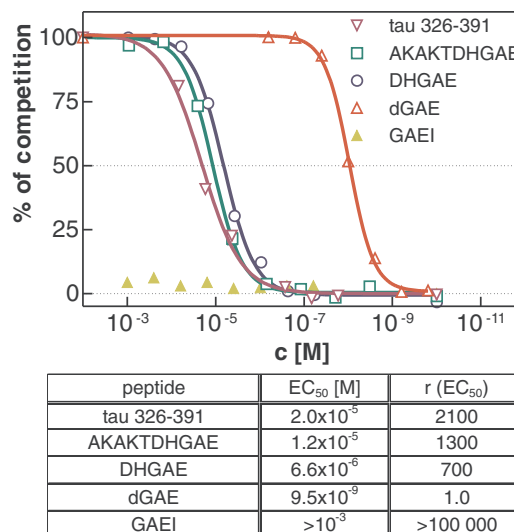


Fig. 2. Contribution of C-terminal component of core PHF subunit to mAb 423 affinity. Figure shows competition between tau C-terminal peptides and core subunit dGAE for binding with mAb 423. Competition curves reflect differences in mAb 423 affinity to respective subunit-derived peptides. Tetrapeptide GAEI represents a negative control lacking measurable reactivity. EC<sub>50</sub> value was used as a measure of affinity; *r* (ratio between EC<sub>50</sub> of respective peptide and EC<sub>50</sub> of dGAE) indicates relative decrease in affinity of mAb 423 to peptide in relation to the full reactivity of subunit dGAE.

specific binding, thus showing that the C-terminus of dGAE directly reacted with structural probe mAb 423. Nevertheless, the affinity of the pentapeptide was 700 times lower than that of the complete subunit dGAE (Fig. 2). Further N-terminal extension of immunoreactive pentapeptide to decapeptide  $^{382}\text{AKAKTDHGAE}^{391}$  or even further upstream until residue 326 (fragment  $\tau_{326-391}$ ) did not increase the affinity. This suggested that region 326–386 was not directly involved in the formation of core PHF subunit structure recognized by mAb 423. Taken together, these findings suggested that the sequence  $^{387}\text{DHGAE}^{391}$  represented whole C-terminal component of the complex structure defined by mAb 423.

### 3.2. Contribution of the N-terminal part of the core PHF subunit to intramolecular folding

Structural analysis of subunit dGAE implicated, in addition to the C-terminal pentapeptide, contribution of N-terminal region (297–325) to the folding of core PHF subunit. In order to identify individual segments essential for this folding, we prepared N-terminal deletion mutants of subunit dGAE.

Four dGAE deletion mutants with different N-termini were constructed and their reactivities with mAb 423 assayed (Fig. 3A). It has been shown [8,16] that variability between six core PHF subunits is restricted to the region corresponding in dGAE to the first nine N-terminal residues (297–305). The mutant ( $\tau_{306-391}$ ) lacking this region showed equal immunoreactivity to that of dGAE (Fig. 3B). This finding showed that residues 297–305 were not essential for assuming 423-specific conformation of core PHF. However, it also indicated that the most significant N-terminal contribution to the core PHF-folding had to be delivered by residues 306–325.

Further N-terminal deletions of core subunit dGAE beyond Ser305 gradually decreased the immunoreactivity of resulting mutants. The mutants  $\tau_{316-391}$  ( $\Delta$  297–315) and  $\tau_{321-391}$  ( $\Delta$  297–320) showed 4.3- and 37-fold decrease in affinity, respectively, when compared to that of full-length core PHF subunit dGAE. Nevertheless, the reactivities of these mutants were still substantially higher than the reactivity of subunit C-terminal pentapeptide  $^{387}\text{DHGAE}^{391}$ . However, further removal of subsequent five residues downstream ( $\Delta$  321–325) yielded the subunit fragment  $\tau_{326-391}$  with weaker binding capacity than that exhibited by pentapeptide  $^{387}\text{DHGAE}^{391}$  (Fig. 3B). Together, these data suggested that region  $^{321}\text{KCGSL}^{325}$  could represent complementary component participating in the formation of folded subunit structure. To test directly whether the sequence  $^{321}\text{KCGSL}^{325}$  was crucial for immunoreactivity and thus to the conformation of the core PHF subunit, we engineered dGAE mutants with internal deletion of individual segments designated as domain I ( $^{306}\text{VQIVYK}^{311}$ ), domain II ( $^{314}\text{DLSKVTS}^{320}$ ) and domain III ( $^{321}\text{KCGSL}^{325}$ ) (Fig. 4A). Surprisingly, deleting domain III (dGAE $\Delta$ III) led to decrease in affinity only about 8-fold, indicating thus significant contribution of either domain I or II to the folding constraints of core PHF subunit (Fig. 4B). Deletion of domain II (dGAE $\Delta$ II) had similar low impact on affinity (about 6-fold reduction) as deletion of domain III. The major destabilizing effect on subunit structure resulted from removing the domain I (dGAE $\Delta$ I), which caused 25-fold decrease in affinity similar to the level of fragment  $\tau_{321-391}$  (Fig. 3). It showed that sequence  $^{306}\text{VQIVYK}^{311}$  had an important contribution in adopting conformational characteristic of core PHF subunit. Nevertheless, none of the examined domains (I, II, III) alone

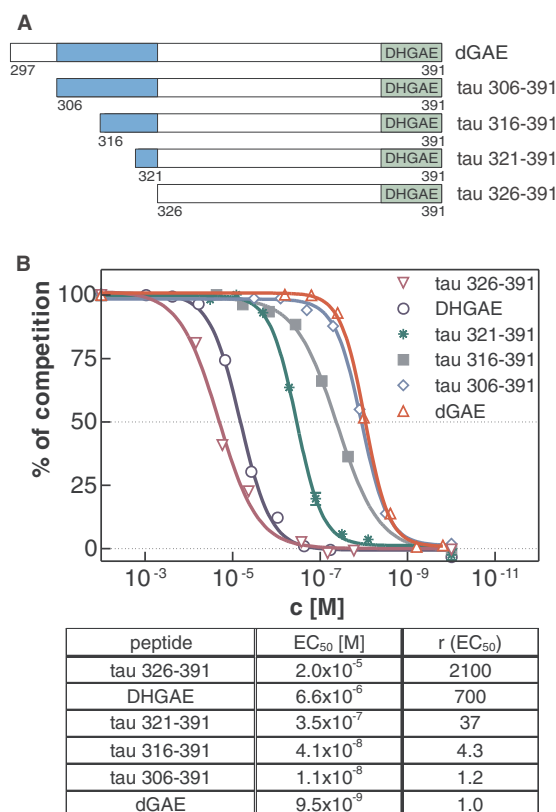


Fig. 3. Identification of N-terminal segment contributing to core subunit conformation. (A) Diagram of N-terminal deletion mutants derived from core subunit dGAE. The region 306–325 important for conformation of core subunit dGAE is colored blue. Position of C-terminal pentapeptide is shown in green. (B) Figure shows competition between N-terminal deletion mutants of dGAE and full-length dGAE for binding with mAb 423. Competition curves reflect differences between subunit mutants in reactivity with mAb 423.  $\text{EC}_{50}$  value was used as a measure of affinity;  $r$  (ratio between  $\text{EC}_{50}$  of respective mutants and  $\text{EC}_{50}$  of dGAE) indicates relative decrease in affinity of mAb 423 to peptide in relation to the full reactivity of subunit dGAE.

exhibited sufficient capacity to reduce the affinity to that of subunit C terminal pentapeptide  $^{387}\text{DHGAE}^{391}$ . These results suggested a local fold encompassed in region 306–325 that could represent the assembled N-terminal component of the conformation recognized by mAb 423 in core PHF subunit. Crucial role in this fold appeared to be assigned to domain I. To prove this possibility, we engineered subunit dGAE mutants which had domain I deleted simultaneously with either domain II [dGAE $\Delta$ (I+II)] or domain III [dGAE $\Delta$ (I+III)]. The decrease in reactivity (23-fold) of the double mutant dGAE $\Delta$ (I+II) was close to that of the mutant lacking the domain I (dGAE $\Delta$ I) (Fig. 4). In contrast, deletion of both domains I and III [dGAE $\Delta$ (I+III)] resulted in dramatic decrease in affinity (650-fold) to the level exhibited by core subunit C-terminal pentapeptide  $^{387}\text{DHGAE}^{391}$ . These findings raised the possibility that the N-terminal component of mAb 423-specific conformation was formed in core subunit by a local fold comprising domains I and III.

### 3.3. Domain arrangement in folded PHF core

Considering the limited size of antigen-binding region of an antibody ( $1000 \text{ \AA}^2$  on average), the C-terminus and N-terminal region 306–325 of core subunit had to be in close proximity to



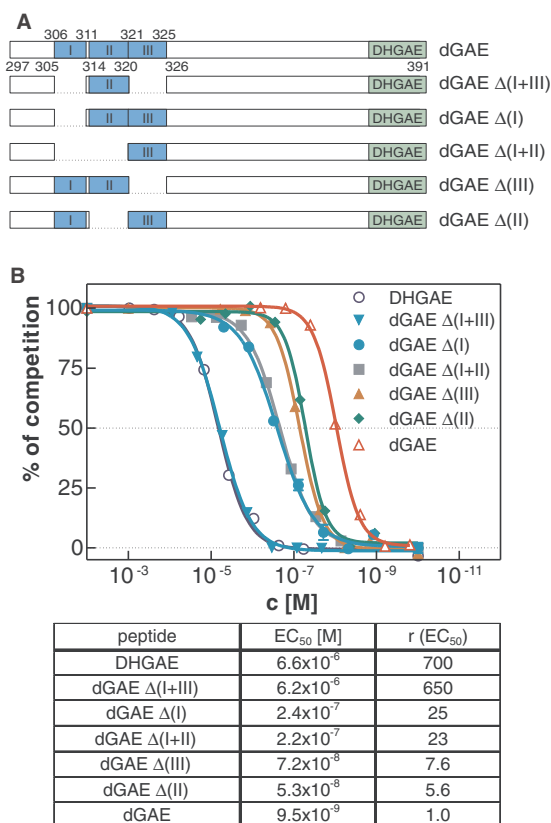


Fig. 4. Role of domains in segment 306–325 contributing to the N-terminal fold of core subunit structure. (A) Diagram of internal deletion mutants derived from subunit dGAE. Positions of domains I, II, III and C-terminal pentapeptide are shown. (B) Competition between deletion mutants of dGAE and full-length dGAE for binding with mAb 423 is shown. Competition curves reflect differences between subunit mutants in reactivity with mAb 423. EC<sub>50</sub> value was used as a measure of affinity; *r* (ratio between EC<sub>50</sub> of respective mutants and EC<sub>50</sub> of dGAE) indicates relative decrease in affinity of mAb 423 to peptide in relation to the full reactivity of dGAE.

each other, provided that core PHF tau adopts a folded structure. Based on this assumption, formation of local N-terminal fold in core PHF subunit could be mediated by direct interaction of domains I and III with C-terminal residues in vicinity or within the pentapeptide <sup>387</sup>DHGAE<sup>391</sup>. The C-terminal component is essential for folding of subunit dGAE, whereas the N-terminal component is only able to contribute when the C-terminal component is engaged. The absolute requirement for glycine at position 389 may indicate an importance of local C-terminal flexibility of subunit for adopting a core PHF conformation [11]. Therefore, the spatial proximity of three subunit segments <sup>306</sup>VQIVYK<sup>311</sup>, <sup>321</sup>KCGSL<sup>325</sup> and <sup>387</sup>DHGAE<sup>391</sup> represents constraints for intramolecular folding of the core PHF subunit. The immunoreactivity of tau deletion mutants with mAb 423 was analyzed also in Western blotting and compared with data from competitive ELISA (Fig. 5). Results from Western blot quantification were consistent with data from ELISA experiments.

It is interesting that polypeptide segments from the overlapping parts of tau molecules, namely residues 312–322 and 305–314, were identified as important contributors to the immunoreactivity of conformational antibodies MC-1 and Tau-66 [10,12]. However, these mAbs have been used for definition

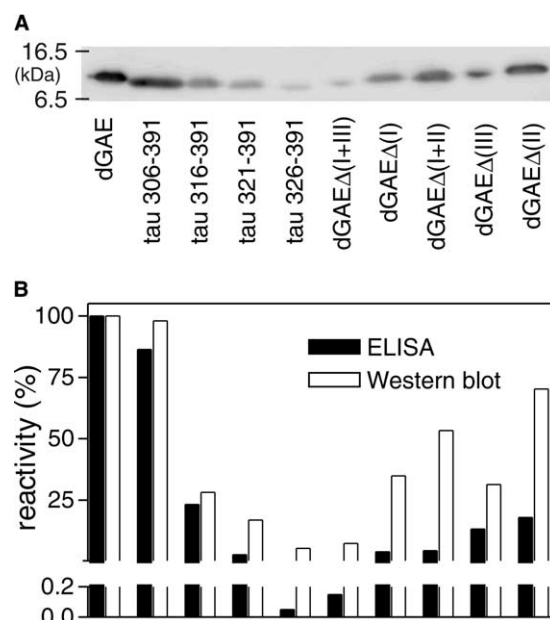


Fig. 5. Quantitative Western blot analysis of the core PHF subunit and its mutants gives results complementary to those obtained by ELISA. (A) 100 ng of individual tau proteins were loaded onto 10–20% gradient SDS-PAGE. Following electroblotting, membrane was stained with peroxidase-labeled mAb 423. (B) Comparison of reactivity in competitive ELISA (expressed as reciprocal EC<sub>50</sub> values) and Western blot reactivity (corrected for molecular weight of individual proteins). All data are normalized to 100% values of dGAE core PHF subunit.

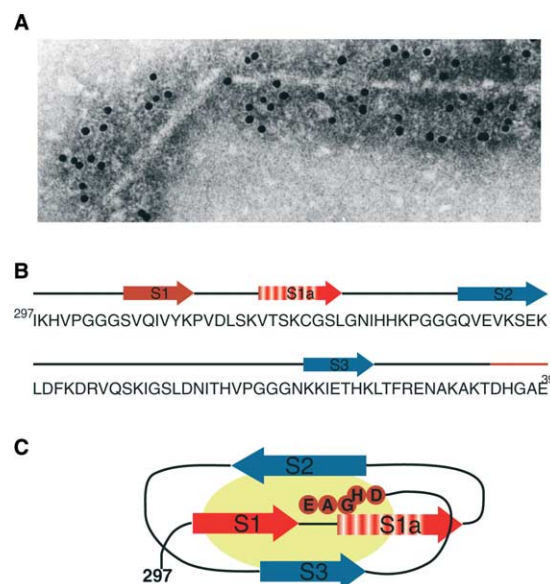


Fig. 6. Folding of subunit core PHF into β-sheet conformation. (A) Immunoelectron microscopy of Pronase-resistant core PHF shows typical immunogold decoration with mAb 423. Pronase-resistant core was isolated and immunodecorated as described [5,6]. PHFs were isolated from AD brain, stage VI, according to Braak [20]. (B) Primary structure of core PHF subunit (dGAE) with individual segments essential for polypeptide folding (red – based on EC<sub>50</sub> values) and with regions of predicted β-strands is shown. (C) Core PHF subunit adopts β-sheet structure. Proposed core structure is based on predicted β-strand propensities and experimental EC<sub>50</sub> values of core PHF specific mAb 423.

of an overall fold of tau molecule before its assembly into PHF. In contrast, the 423 was raised against already folded core PHF and therefore could disclose tau conformation responsible for PHF stability. Taking together, requirement for the third microtubule-binding region of tau is common denominator for immunoreactivity of conformational antibodies MC-1, Tau-66 and 423. This indicates the fundamental role of this region in both PHF genesis and its stabilization. The constraints that determine dGAE subunit folding appear to be characteristic of an assembled configuration of core PHF tau in AD. Based on these findings, we present a model depicting folding of the core PHF subunit, dGAE, in which we propose the formation of  $\beta$ -sheet (Fig. 6) with domain I and/or III acting as an intramolecular zipper for  $\beta$ -sheet formation. Such conformation of dGAE could represent binding interface for assembly of core unit (dGAE) into core PHF. The work represents first information on subunit core PHF folding and would contribute to deciphering the molecular mechanism of PHF assembly.

**Acknowledgements:** We gratefully acknowledge Dr. Gustav Russ (Institute of Virology, Bratislava, Slovakia) for helpful discussions and careful reading of the manuscript and Dr. L. Vechterova (Institute of Neuroimmunology) for help with western blotting.

## References

- [1] Novak, M., Ugolini, G., Fasulo, L., Visintin, M., Ovecka, M. and Cattaneo, A. (1999) in: *Alzheimer's Disease and Related Disorders; Etiology, Pathogenesis and Therapeutics* (Iqbal, K., Swaab, D.F., Winblad, B. and Wisniewski, H.M., Eds.), pp. 281–291, John Wiley & Sons Ltd, New York.
- [2] Goedert, M. and Klug, A. (1999) *Brain Res. Bull.* 50, 469–470.
- [3] Grundke-Iqbal, I., Iqbal, K., Tung, Y.C., Quinlan, M., Wisniewski, H.M. and Binder, L.I. (1986) *Proc. Natl. Acad. Sci. USA* 83, 4913–4917.
- [4] Alonso, A.C., Zaidi, T., Grundke-Iqbal, I. and Iqbal, K. (1994) *Proc. Natl. Acad. Sci. USA* 91, 5562–5566.
- [5] Wischik, C.M., Novak, M., Edwards, P.C., Klug, A., Tichelaar, W. and Crowther, R.A. (1988) *Proc. Natl. Acad. Sci. USA* 85, 4884–4888.
- [6] Wischik, C.M. et al. (1988) *Proc. Natl. Acad. Sci. USA* 85, 4506–4510.
- [7] Uversky, V.N. (2002) *Protein Sci.* 11, 739–756.
- [8] Novak, M., Jakes, R., Edwards, P.C., Milstein, C. and Wischik, C.M. (1991) *Proc. Natl. Acad. Sci. USA* 88, 5837–5841.
- [9] Jicha, G.A., Lane, E., Vincent, I., Otvos Jr., L., Hoffmann, R. and Davies, P. (1997) *J. Neurochem.* 69, 2087–2095.
- [10] Jicha, G.A., Berenfeld, B. and Davies, P. (1999) *J. Neurosci. Res.* 55, 713–723.
- [11] Khuebachova, M., Verzillo, V., Skrabana, R., Ovecka, M., Vaccaro, P., Panni, S., Bradbury, A. and Novak, M. (2002) *J. Immunol. Methods* 262, 205–215.
- [12] Ghoshal, N., Garcia-Sierra, F., Fu, Y., Beckett, L.A., Mufson, E.J., Kuret, J., Berry, R.W. and Binder, L.I. (2001) *J. Neurochem.* 77, 1372–1385.
- [13] Mena, R., Wischik, C.M., Novak, M., Milstein, C. and Cuellar, A.C. (1991) *J. Neuropathol. Exp. Neurol.* 50, 474–490.
- [14] Novak, M., Wischik, C.M., Edwards, P., Pannell, R. and Milstein, C. (1989) *Prog. Clin. Biol. Res.* 317, 755–761.
- [15] Jakes, R., Novak, M., Davison, M. and Wischik, C.M. (1991) *EMBO J.* 10, 2725–2729.
- [16] Novak, M., Kabat, J. and Wischik, C.M. (1993) *EMBO J.* 12, 365–370.
- [17] Goedert, M., Spillantini, M.G., Jakes, R., Rutherford, D. and Crowther, R.A. (1989) *Neuron* 3, 519–526.
- [18] Csokova, N., Skrabana, R., Liebig, H.-D., Mederlyova, A., Kontsek, P. and Novak, M. (2004) *Protein Expression Purification* 35, 366–372.
- [19] Nunn, D.L. and Taylor, C.W. (1990) *Biochem J.* 270, 227–232.
- [20] Braak, H. and Braak, E. (1991) *Acta Neuropathol. (Berl)* 82, 239–259.